The Mechanism of Shrimpoluminescence

Tyler C. Sterling*

(Dated: January 18, 2022)

I. INTRODUCTION

Snapping shrimp, like our cute friend in fig. 1, produce cavitating bubbles by snapping their claws [1–3]. They have a strong appendage called the *dactyl* (fig. 1 [center]) that is used to create a high-velocity jet of water. The low pressure region in the jet's wake forms a bubble (fig. 1 [right]) that, when it collapses, produces a noise loud enough to be detected over a mile away [4]. The noise produced by groups of shrimp is so intense that the U.S. Navy used them as "sonar-camouflage" in the Pacific ocean during World War II [1]. The shrimp were not patriots helping the war-effort, however; they snapped for food. The sound wave produced by the cavitating bubble is used to stun or kill prey [1]. If the shrimp's prey had very[1] sensitive eyes (and also were not dead) they might notice a flash of light is also produced through an effect referred to as "shrimpoluminescence" in the case of the pistol shrimp [2], but more generally known as *sonoluminescence*.

Sonoluminescence (SL) is defined as the process by which a "driven gas bubble collapses so strongly that the energy focusing at collapse leads to light emission" [5]. SL comes in two forms:

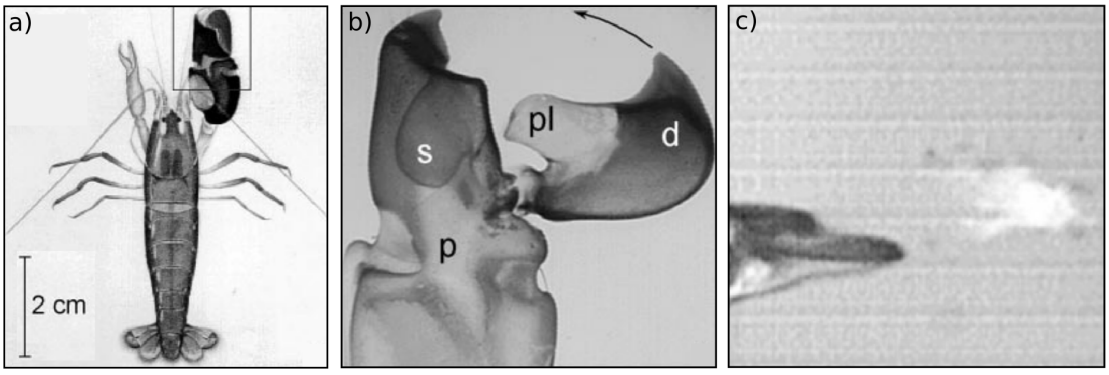

FIG. 1. (left) Snapping shrimp (*Alpheus heterochaelis*). (center) Blown-up view of the shrimp's claw. The *plunger* (pl) on the *dactyl* (d) rapidly enters the *socket* (s), ejecting a high-velocity jet of water. A time near the bubble collapse is shown on the right. The light emission is too dim to be seen by the naked eye. Adapted from refs. [1] and [2].

* ty.sterling@colorado.edu

[1] Shrimpoluminescence is too weak to be seen by the naked-eye.

(i) single-bubble sonoluminescence and (ii) multi-bubble sonoluminescence. Multi-bubble sonoluminescence (MBSL) consists of "the simultaneous creation and destruction of many separate, individual cavitation bubbles" [5, 6], whereas in single-bubble sonoluminescence (SBSL), rather obviously, only a single bubble is present [7].

MBSL was discovered by accident in 1933 when engineers who were trying to accelerate photo-development noticed that a photo-sensitive plate immersed in an "insonated" fluid became foggy from exposure to light [8, 9]. This result was not particularly important at the time since there was no practical use for the light emission and it was already known that cavitating bubbles, e.g. those generated by the sound field, could do trememdous damage to ship's propellers. The discovery's impact is summarized by Brenner: "if the cloud [of cavitating bubbles] collapses violently enough to break molecular bonds in a solid, why should it *not* emit photons" [5]. The theory of caviation was already quite mature. Euler (as early as 1754) hypothesized that if the velocity in a fluid was large enough, negative pressures could become so large as to "break the fluid" [7, 10]. In the early 1900's, Lord Rayleigh wrote down and solved the differential equation for a vapor filled cavity collapsing in water (the so-called Rayleigh equation), giving the first rigorous theoretical treatment of cavitation [11, 12]. He found that the bubble wall diverges during collapse, giving rise to "cavitation". Since then, the theory of *bubble dyanmics* has been refined considerably and we will devote a large portion of the paper to it [5, 12–15].

Still, very little information was accessible about the light emission until the 1990's when it was discovered that stable [2], single bubbles could be created and driven to emit light in SBSL [6, 7, 16]. SBSL, unlike previous studies on MBSL, allowed very precise control and measurement of the SL process. Practically all progress on understanding SL in general has been based on SBSL, with some authors even calling it "the hydrogen atom of sonoluminescence" [6, 17]. Light emission from an isolated bubble is not complicated from scattering off other bubbles. Similarly, the bubble is not perturbed by interaction with other bubbles or, due to its tiny extent, by interaction with the container walls. Both theory and experiments are greatly simplified compared to MBSL. Measurments of the SBSL spectrum resulted in a nearly featureless continuum, leading to speculation that the light emission was very high-temperature thermal radiation [18, 19]. Around the same time, it was found that the light pulse was orders or magnitude shorter than the time in which the bubble was compressed to its smallest radius [15, 20]. This discovery implied that SL was nearly decoupled from the bubble's dynamics and models were proposed based on *converging shock*

[2] *Stable* is compared with *transient* when discussing cavitation. A stable bubble persists through multiple cycles of cavitation, oscillating non-linearly around an equilibrium size. Transient bubbles appear and then collapse to disappear

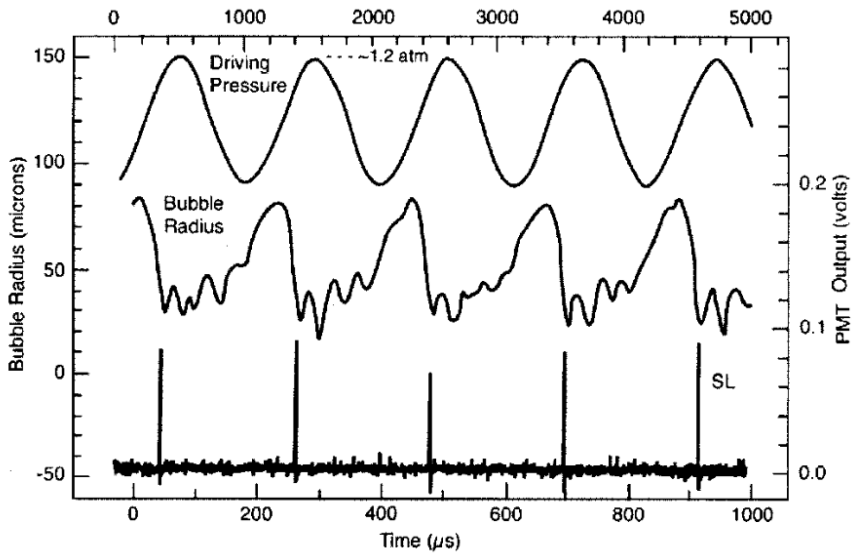

FIG. 2. Driving pressure, bubble radius, and SL intensity as a function of time for an air bubble in water. Note that the width of the light pulse at bubble collapse is *very* short. From ref. [6]

waves at the bubble's center with estimates of the temperature at the center of bubble at $\sim 10^8$ K [21, 22]. These very high estimates for the temperature in the bubble finally led to a spark of interest more broadly: if the temperature in the bubble were really that large, then it should be possible for nuclear *fusion* to occur. An action movie featuring Keanu Reeves was made with this concept at the center of the plot [3]. and in the early 2000's, several papers were published claiming that stable nuclear fusion was possible in the lab using a method based on SBSL []. Unfortunately these studies turned out to be fraud and evidence eventually emerged that shape instabilities prevent converging shock-waves, severely reducing estimates for the temperature to $\sim 10,000$ K [5]. Current estimates for the temperature, which we will study in the rest of this paper, put the center of a sonoluminescing bubble between $10,000 - 30,000$ K [23**?** –27].

Let us now sketch SBSL more precisely. An air bubble is trapped at the center of an acoustically driven flask containing a fluid. The pressure wave in the fluid, shown as a function of time in the top curve in fig. 2, drives the expansion and contraction of the bubble and, in turn, the gas in the bubble responds to the bubble's oscillations. Under the right circumstances, we get the very complicated non-linear response of the bubble's radius shown in the middle curve in fig. 2. Now let's see how these dynamics lead to SBSL. First, as the pressure decreases and becomes negative, the bubble expands gradually: surface tension and the negative pressure in the bubble tend to slow this down. Eventually the pressure is increasing again. Once it becomes positive, the bubble

[3] It is called *Chain Reaction* and I am unwilling to watch it.

violently collapses to its minimum radius: during compression, the negative pressure in the bubble is very large and works with the driving pressure to rapidly accelerate the bubble's wall. The collapse is so fast that the bubble's contents are adiabatically compressed, resulting in a very large temperature in the bubble. If everything is just right, the temperature is large enough that a pulse of light is produced as shown by the bottom curve in fig. 2. After the collapse, there is a period of *after-bouncing* that continues until the pressure is negative again.

It turns out that the light pulse is very short (only $\sim 0.003\%$ of the bubble's cycle [24]) and its spectrum depends sensitively on both the mechanical and chemical properties of the host-liquid and gas in the bubble, as well as the driving pressure and frequency [5, 24]. The mechanical properties determine the pressure and temperature in the bubble which in turn control chemical reactions: all of these data are used to explain the light emission. For extreme enough conditions in the bubble, which occur only briefly, molecular dissociation and recombination, atomic/excited-state transitions, and electron-ion/electron-neutral atom bremsstrahlung are possible [23–28]. These are now known to be the processes which emit light [17, 29].

Our goal in this paper is to present the simplest theory needed to understand shrimpoluminescence, though we will specialize to the related physics of a bubble undergoing SBSL in the lab as it is apparently simpler to create and characterize SBSL without involving shrimp[4]. Firstly, we will look at the problem of the fluid containing the bubble and derive the equations of motion for the bubble's wall. Nextly, we will use our results for the bubble's wall to understand the dynamics of the gas trapped in the bubble, estimating the *temperature* and *pressure* along they way. Finally, we will discuss theories presenting the mechanisms of light emission/absorption in the bubble which, combined with the temperature, allow use to calculate the bubble's light spectrum. Throughout the course of our journey, we will stick to the simplest results that still contain the essential physics we need. Connections to more advanced treatments, and their implications, are provided for completeness.

II. BUBBLE DYNAMICS

In this section, we present the theory needed to model the dynamics of a bubble undergoing SBSL. We will split this into parts. First, we will derive the equations of motion for the bubble's wall. Next, we will review some important experimental developments that we will then use to

[4] For example, convincing the shrimp to snap requires tickling them [1, 2, 17]. Besides notable exceptions [3], practically all work to study SL has not involved shrimp.

argue for a simple model for the dynamics of the gas in the bubble. Lastly, we will compare results of a simulated bubble to experimental data. The connection to experiment will be what allows us to calculate the temperature in real bubbles.

A. The Bubble Wall

It turns out the dynamics in SBSL are quite well described both qualitatively and quantitatively by the classical theory of bubble dynamics [5, 12, 13, 24, 29–31]. The starting point for the theory is Rayleigh's original work [11], now expounded upon by many others. The most widely known modern work is that of Plesset [12, 30, 32], resulting in the so called "the Rayleigh-Plesset" (RP) equation. The field of bubble dynamics is quite mature and attempting to review it here would be out of scope of this paper; instead, the reader is referred elsewhere [5, 13, 29, 30].

With suitable approximations, the RP equation is deduced from the *Navier-Stokes* equations [5, 12, 13, 24, 29, 30]. We assume the host liquid is incompressible, ultimately resulting in neglecting effects of sound radiated by the bubble. We also assume irrotational flow so that there is only radial motion in the liquid, i.e. $\boldsymbol{u} = u\boldsymbol{r}$ is the fluid's velocity with u the speed and $\boldsymbol{r}$ the radial unit-vector. For irrotational flow, we can represent the velocity as the gradient of a scalar function: $u\boldsymbol{r} = (\partial_r \phi)\boldsymbol{r}$ [33]. This amounts to assuming that the bubble is always spherical which seems like a rather drastic approximation but is validated experimentally. The fact that the bubble tends to remain spherical is understood by accounting for surface-tension at the liquid-bubble interface [13].

Next, we assume that *viscosity* is negligible in the bulk dynamics of the liquid which, in low viscosity fluids such as water which, is an accurate approximation [5, 12, 13, 30]. We will account for viscosity later when looking at the bubble-liquid interface. We will also assume reversible and isothermal flow, i.e. no damping and no heat flow between fluid parcels. The pressure p is determined from an instantaneous equation-of-state, $p = p(\rho, T)$, with ρ the density and T the temperature. In the case of SBSL, this is valid since the bubble makes up a *tiny* fraction of the total volume and any heat-transport across the liquid-bubble interfacing is negligible [13]. Related to the fact that the bubble is tiny, we assume that the extent of the liquid is so large compared to the bubble that we may consider the dynamics of the liquid as if there were no bubble present; similarly, we consider the dynamics of a bubble in an infinite, isotropic medium. Of course the bubble-liquid interface enters both systems as a boundary condition.

With these simplifying assumptions the Navier-Stokes equations for the fluid are [13, 30, 31, 34]

$$\begin{aligned} \partial_r \left[\partial_t \phi + \frac{1}{2} (\partial_r \phi)^2 \right] &= -\frac{1}{\rho} \partial_r p \\ \partial_t \rho + \partial_r \phi \partial_r \rho + \rho \partial_r^2 \phi &= 0. \end{aligned} \tag{1}$$

The first equation is conservation of momentum; the second is mass-continuity. We can integrate the first equation using the fact that the compressibility is negligible [34]. On the left side, we take the velocity to vanish at infinity. On the right side, we assume that only the static and driving pressures, p_∞ and $P(t)$ respectively, are relevant so that [13, 30, 34]

$$\partial_t \phi + \frac{1}{2} (\partial_r \phi)^2 = \frac{(p_\infty + P(t)) - p(t, r)}{\rho}. \tag{2}$$

Now let us assume that the velocity potential satisfies a wave equation $\nabla^2 \phi - (1/c^2) \partial_t^2 \phi = 0$ with c the speed of sound in the fluid [5]. Again, we use incompressibility by recalling that for an incompressible fluid $c \to \infty$ which implies $\nabla^2 \phi = 0$ [13, 30, 34]. Then we can ignore retardation effects and write the solution of $\nabla^2 \phi$ as $\phi = \psi(t)/r$ with ψ a time-dependent coefficient. The boundary condition for the velocity at the bubble wall, $u(R) \equiv \dot{R}$ with R the bubble radius, gives $\psi = -R^2 \dot{R}$ and $\phi = -R^2 \dot{R}/r$. Plugging this into the left hand side of eq. 2 and evaluating at the bubble wall, we arrive at the Rayleigh-Plesset equation [12, 13, 30, 32, 34]

$$R \ddot{R} + \frac{3}{2} \dot{R}^2 = \frac{p_B(t) - (p_\infty + P(t))}{\rho} \tag{3}$$

with $p_B \equiv p(r = R, t)$ the pressure in the fluid at the bubble wall. The combination $p_\infty + P(t)$ is the ambient pressure [13, 30] which gives the pressure in the fluid in the absence of the bubble. The left hand side of eq. 3 may be regarded as the kinetic energy (density). The right hand side is the change in enthalpy (density) due to the fluctuating bubble, i.e. the dynamics of the bubble given on the left hand side are determined by the enthalpy in the fluid due to the bubble's motion. In deriving this equation, we have assumed that the speed of propagation in the fluid is infinite. In reality, this is not true but this approximation will be very good close to the bubble (in the *near-field*) where retardation effects are negligible anyway. In a similar way, we have assumed that the energy in the fluid due to distorting its volume is negligible. This approximation will be accurate near the bubble as well since the kinetic energy in this region will dominate [13].

Eq. 3 can be refined a little further. Since the motion in the fluid is purely radial, we expect the only relevant stresses to be normal to the bubble wall. The normal stress combined with the

[5] This doesn't come from thin air. We could write the r.h.s. of eq. 2 as the enthalpy, $h \equiv \int dp/\rho$, and similarly introduce $dh = dp/\rho$ in the second line of eq. 1. Eliminating h between the two and dropping small terms $\sim u/c$, we arrive at the homogeneous wave equation [5, 13, 34].

pressure in the gas, $p_g(t)$, gives us [5, 13, 30, 34]

$$p_B(t) = p_g(t) - \frac{1}{R}\left(2\sigma + 4\eta\dot{R}\right). \tag{4}$$

The term $\sim \sigma$ is called the *Laplace pressure* and is from surface tension. The $\sim \eta$ term is due to the *bulk viscosity* in the fluid. The RP equation becomes

$$R\ddot{R} + \frac{3}{2}\dot{R}^2 = \frac{1}{\rho}\left[\Delta p(t) - \frac{1}{R}\left(2\sigma + 4\eta\dot{R}\right) - P(t)\right] \tag{5}$$

with $\Delta p = p_g(t) - p_\infty$ the deviation of the pressure inside the bubble from the static pressure. With the above assumption that the compression is adiabatic, the conditions inside the bubble are decoupled from the liquid (besides the coupling through the RP equation) and we may regard $p_g(t)$ in the bubble as a given quantity to be determined from an equation of state. Recall $P(t)$ is the time-dependent part of the pressure in the absence of the bubble: we may regard this as an external pressure from e.g. a driving stress. In SBSL, this is from the transducers driving the flask and $P(t)$ is an acoustic plane wave. Keller and coworkers showed that the modification required to the RP equation is the replacement $P(t) \to P_0 \sin(\omega t)$ [35].

The RP equation (eq. 5) is pretty but its analytical solution is intractable. Direct solutions of the RP equation or its variants are done numerically using e.g. Euler or Runge-Kutta methods [29, 36]. It is no great challenge computationally. For now, let's see what we can understand analytically by making some more approximations. If we linearize in the bubble's radius $R(t) \approx R_0\,(1 + x(t))$ with $x(t) \ll 1$, we can derive a forced harmonic oscillator equation for $x(t)$ [29, 31]. However the low driving amplitude regime where this method is valid is irrelevant to SBSL so we won't pursue it here. Instead, we can look at the interval where the bubble wall's velocity is very large, called *The Rayleigh Collapse*; the right hand side of eq. 5 will be much smaller than the $\dot{R}^2$ term and we may neglect it [5, 11, 13, 32]. Rayleigh looked at the same problem, i.e. a cavitating void in water:

$$R\ddot{R} + \frac{3}{2}\dot{R}^2 = 0 \tag{6}$$

and found the solution to be $R(t) \sim (t_* - t)^{2/5}$ [5], with t_* the time of collapse. The velocity, $\dot{R} \sim (t_* - t)^{-3/5}$, diverges as the bubble collapses. This observation is what lead to Rayleigh's argument for the origin of cavitation damage to ship's propellers.

In reality, the bubble's velocity does not become infinite and, in the case of *stable* SBSL, the radius remains finite at all times. In the full RP equation (eq. 3) the only term capable of compensating the bubble wall's motion is the diverging pressure inside the bubble itself [5]. If we had not assumed incompressibility, eq. 3 would include a term arising from the sound radiation

from the bubble itself. A family of solutions, collectively called "Rayleigh-Plesset equations," are derived in this way [30, 37–39]. It turns out that the most important term for slowing the bubble wall's diverging velocity is $\propto \dot{p}_g$. Keeping only this term provides the most popular variant of the RP equation [14, 40]. This equation is only slightly more complicated than the RP equation (eq. 5), the only change being the added term $\propto \dot{p}_g$ which is determined from solving the decoupled problem of the gas inside the bubble. The observed error between this equation and experiment is only significant in the interval during bubble collapse and even still, results of solving this equation are quantitatively in good agreement with measurements of the bubble's radius [5].

Above, we assumed that the bubble always remains spherical. Of course this isn't always true and *shape-instabilities* occur for the right combinations of mechanical properties and driving force/frequency. Usually shape-instabilities destroy the bubble and kill SBSL so we won't focus on these isues here. We will always assume we are in a parameter-regime where SBSL occurs. The reader is referred to one of several reviews on the *phase-space* of SBSL for more info [5, 25, 29, 41].

B. The Bubble's Interior

The theoretical progress on the bubble's interior since the discovery of SBSL in the late 1990's [7] follows two paths [5, 24, 29]: (i) model calculations based on the RP equations and an equation of state for the pressure (from which we may calculate the temperature) are used to try to reproduce the easily measurable dynamics of the bubble. (ii) We can model the light emission itself and compare our calculation to spectroscopic measurements of SBSL [5, 18].

Most early progress on the bubble's interior depended on the former method: if we predict the right dynamics, then we might know the correct pressure and temperature in the bubble. These data are then used to try to describe the light emission. Calculating the dynamics of the bubble's wall from one of the RP equations (e.g. eq. 5) requires the pressure inside the bubble as input. We would like to find a suitable form for $p_g(t)$ in the RP equations that reproduces the measured radius-time curve $R(t)$ for a stable cavitating bubble. It turns out that this is a very complicated problem: gas diffusion and rectification (one-directional diffusion) between the bubble and liquid vary the number of particles present and, to make things worse, the conditions inside the bubble facilitate chemical reactions between the air and water-vapor changing the properties of gas dynamically [5]. Brenner et. al elegantly summarized the significance of this problem [5]: "one of the exciting features of modern research on SBSL is that it is a testing ground for how well mathematical models can deal with such a complicated situation"

The other method to understand the bubble's interior is its light spectrum. For the first decade or so, SBSL experiments were done using water as the liquid medium [5, 7, 24]. Careful measurements of the emission from SBSL in water resulted in an almost featureless spectrum and attempts to fit it as black-body radiation were not sucessful [18]. Little progress was made on this front for quite some time [5]. The utility of analyzing the light spectrum of SBSL in water is succinctly described by Suslick [24]: "because of the inherent ambiguity associated with the analysis of featureless spectra of unknown origin, a more rigorous explanation is unlikely to be generated".

Some attempts were made to measure SBSL using non-aqueous host liquids e.g. alcohols, silicone oils [40, 42], but experiments with air bubbles were not very successful [40]. Eventually, different gases were tried in water. Recall, air is $\sim 80\%$ N_2, $\sim 20\%$ O_2, and $\sim 1\%$ Ar. Considering the relatively large content of O_2 and N_2, degassed water *regassed* with N_2 or O_2 or a mixture were checked first and found not to produce SBSL [19]. What was discovered was that a small amount of noble-gas was required for SBSL to occur [5, 19, 40]. A result of this work was the *argon rectification hypothesis* [5, 24, 29, 43]. The hypothesis claims that all species in the air inside the bubble besides argon are gradually ejected from bubble's interior until all that remains is pure argon. The theory is based on the fact that, at the elevated temperatures and pressures inside the bubble, dissociation of O_2 and N_2 into radicals is possible. These species then react with the water vapor radicals to form species that are soluble in the host fluid. As the pressure becomes very large during the compression stage of SBSL, the soluble materials leave the bubble and do not re-enter since their solubility in water is enormous compared to the Ar content of the bubble [43]. Over many cycles, the contents of an air bubble in water become nearly pure argon. Moreover, it was hypothesized that the SL would be much more intense when the contents of the bubble are a pure inert gas: if the contents were e.g. molecules, bond breaking/formation would alter the pressure of the gas, ultimately reducing the temperature and reducing the amount of light production [5, 17, 24, 29]. This mechanism has been used to explain the relatively weak light, i.e. the low temperature, in MBSL: the bubbles are transient and cannot remove a significant amount of O_2 or N_2 over a single cycle. The current belief is that the contents of a bubble undergoing SBSL in water are (nearly) pure argon after $\sim 10^3$ cycles [5, 29].

Still, most studies continued to use water as the host liquid until it was realized that SBSL in aqueous H_2SO_4 produces light 10^3 times brighter than in water, allowing more precise measurements of the light spectrum [23, 28]. The mechanical properties in aqueous H_2SO_4 allow stable SBSL with a larger bubble radii than in water, increasing the emitting volume. More importantly, new measurements revealed the phase space of SBSL in aqueous H_2SO_4 included a much larger

range of pressure than water. SBSL in aqueous H_2SO_4 could be driven at very low pressure, leading to much lower temperature bubbles, while driving at large pressure led to conditions similar to SBSL in water.

Careful experiments revealed that the spectrum depended critically on the noble-gas content and driving pressure. Suslick et. al measured the different emission spectra from Ar, Xe, and Kr bubbles in aqueous H_2SO_4, driven to have similar conditions to those in an air bubble in water [23, 24, 28]. Importantly, they were able to identify spectral lines from Ar^+, Xe^+, and Kr^+ excited state transitions, proving that the core of the bubble is plasma. Perhaps equally as crucially, they found the absence of emission lines from components of aqueous H_2SO_4 vapor [24, 28]: the plasma contained only the noble-gas, experimentally confirming the argon rectification hypothesis. The spectra at different pressures were in very good agreement with detailed calculations of emission from noble-gas plasmas [25, 26]. This work also explained why the spectrum in water is featureless (i.e. has no emission lines). The larger pressure in SBSL in water results in an increased collision rate between particles, broadening the spectral lines [23–25, 28].

This argon rectification hypothesis greatly helped to refine models for the gas dynamics in the bubbles and confirmed why simple models usually work well [5, 24]. With this in mind, we choose only to focus on results known to be relevant to the dynamics of a bubble undergoing SBSL. Excellent books and modern reviews on modeling the gas dynamics exist elsewhere [5, 29, 31]. We will hold off on discussing the plasma until a later section.

C. Gas Dynamics

Of course the most straightforward way to model the gas dynamics in the bubble is through direct solution of the Navier-Stokes equations for the gas [5]. In fact, serious quantitative predictions of the conditions of the bubble's interior still take this path [23, 25–28]. Equations of motion with varying degrees of sophistication are derived for the gas and the system of gas dynamical equations and the RP equations are solved numerically. The discussion proceeds in much the same way as deriving the RP equations above but is slighlty more complicated [5, 29], so we will omit it. Instead, let us look at a simple model and discuss how it can be extended to more acurately represent the dynamics.

Recalling that the bubble is (almost) purely noble-gas, a simple but reasonable model for the gas dynamics, at least during the collapse, is that of an adiabatically, quasistatically compressed Van der Walls gas [5, 14, 40, 44, 45]. In the context of SBSL, the interaction term in the Van

der Walls (VdW) equation of state is usually neglected and the only modification to the ideal gas result is the excluded volume of the real gas molecules, $V_h = 4\pi h^3/3$, with h the VdW *hard-core radius*. The pressure in an adiabatically compressed *ideal* gas at volume V_2 is [46]

$$P_2 = P_1 \left(\frac{V_1}{V_2}\right)^{\gamma} \tag{7}$$

where P_1 is the initial pressure at volume V_1 and $\gamma = C_P/C_V$ is the ratio of the constant-pressure and constant-volume specific heats respectively. In our case, we assume that our bubble has an ambient radius R_0 where the pressure is at its equilibrium value, p_0. The ambient volume of the bubble is $V_0 = 4\pi R_0^3/3$. We know that $p_0 = p_\infty + 2\sigma/R$ from earlier. We want to calculate the pressure in the gas, $p_g(t)$, as a function of the bubble's instantaneous radius $R(t)$ determined from an RP equation (e.g. eq. 5). Plugging these into eq. 7, and subtracting the excluded volume, we arrive at a very commonly used equation in the context of SBSL [5, 14, 40, 44, 45, 47]:

$$p_g(t) = \left(p_\infty + 2\frac{\sigma}{R_0}\right)\left[\frac{R_0^3 - h^3}{R^3(t) - h^3}\right]^{\gamma} \tag{8}$$

It's clear that the purpose of the excluded volume is to make sure that if the bubble collapses so strongly that its contents become incompressible (i.e. $R(t) \to h$), the pressure diverges [5, 44]. Eq. 8 can be inserted into an RP equation which can then be integrated numerically to determine the bubble's complete dynamics for all time.

Our physical intuition tells us why eq. 8 is sensible during the bubble's collapse: the bubble wall's velocity is fast and very little heat can flow out during compression. During the expansion and after-bounce stages of the bubbles cycle, which comprise its majority, the gas dynamics should instead be regarded as *isothermal* [5]. This is true because, when the bubble's velocity is on the order of the heat diffusion timescale, the temperature throughout the bubble is nearly equal to that in the liquid [5, 13, 29]. The relevant modifications to eq. 8 turns out to be replacing $\gamma \to 1$. A neat way of including both isothermal and adiabatic gas dynamics is continuously varying the exponent, γ in eq. 8, between its adiabatic and isothermal values, C_P/C_V and 1, respectively. This technique has been commonly used in calculations of SBSL in water [5, 30, 41, 45]. These simple forms, even using the constant adiabatic exponent $\gamma = 5/3$, give close to the correct bubble dynamics (see fig. 4) with more advanced solutions using the full gas dynamical equations improving only on estimates for the conditions inside the bubble [5, 29].

Recalling that one of main goals of modeling the bubble dynamics in SBSL was to calculate the temperature inside the bubble, we can also derive an an equation for $T(t)$ [5, 40, 47]:

$$T(t) = T_0 \left(\frac{R_0^3 - h^3}{R^3(t) - h^3}\right)^{\gamma - 1}. \tag{9}$$

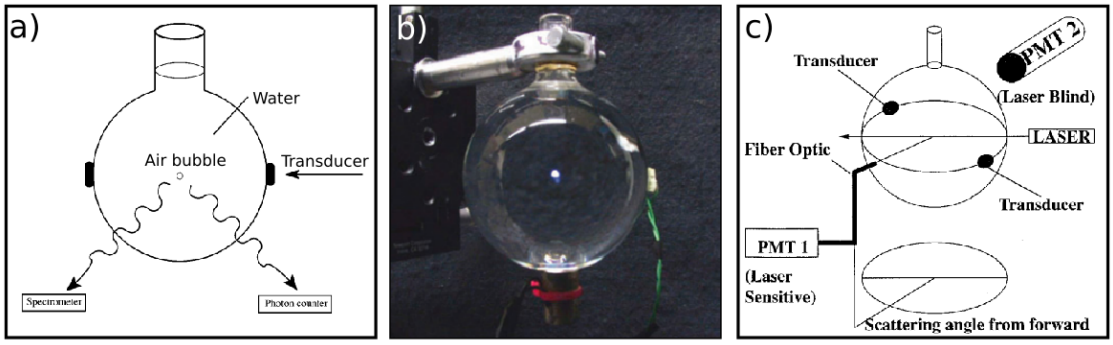

FIG. 3. (a) Schematic of a spherical "acoustic levitation cell". The piezoelectric transducers that drive the bubble trapped in the flask are labeled in the diagram. (b) Photograph of the same. Here, the fluid is aqueous H_2SO_4 instead of water. A sonoluminescing bubble is clearly visible in the center of the flask. The photo was taken in a fully lit room with exposure time 2 s. (c) Schematic of a Mie scattering experimental setup. A similar levitation cell as (a) is shown with an added laser source and photomultiplier tubes (PMT) to analyze the scattered and emitted light. (a), (b), and (c) are from refs. [5], [24], and [48] respectively.

Earlier, we said that during the bubble's after-bounces and expansion, the gas dynamics is isothermal; then we take T_0 to be the temperature of the liquid. An RP equation, e.g. eq. 5, combined with the gas dynamical equation, eq. 8, and the known liquid and gas properties η, σ, and h, can be used to calculate the dynamics of an acoustically driven bubble, giving us the time-dependence of the pressure and temperature in the bubble.

III. BUBBLES IN THE LAB

Creating stable, single bubbles in a laboratory experiment is not particularly challenging and can be done with standard and low-cost materials. A typical experimental setup is shown in fig. 3. Since we are concerned with explaining the light emission process itself, we will only sketch the experimental setup; it can be summarized as follows [5, 7, 16, 24, 29, 31, 48, 49]. A suitable sample of liquid is placed into a flask. Stuck to the outside are piezoelectric transducers driven sinusoidally to excite an acoustic resonance of the flask: a typical flask is a few cm across with a resonance at ≈ 20 kHz [5]. The frequency is chosen to form a pressure *antinode* at the center of the flask, trapping a bubble there.

The driving pressures relevant to SBSL (~ 1.5 atm) are too small to cause bubbles to form spontaneously [5]. Instead, a bubble is usually *seeded* somehow. In the original work of Gaitan, an air bubble was injected using a syringe [7]. More recently, seeding methods involve shooting a

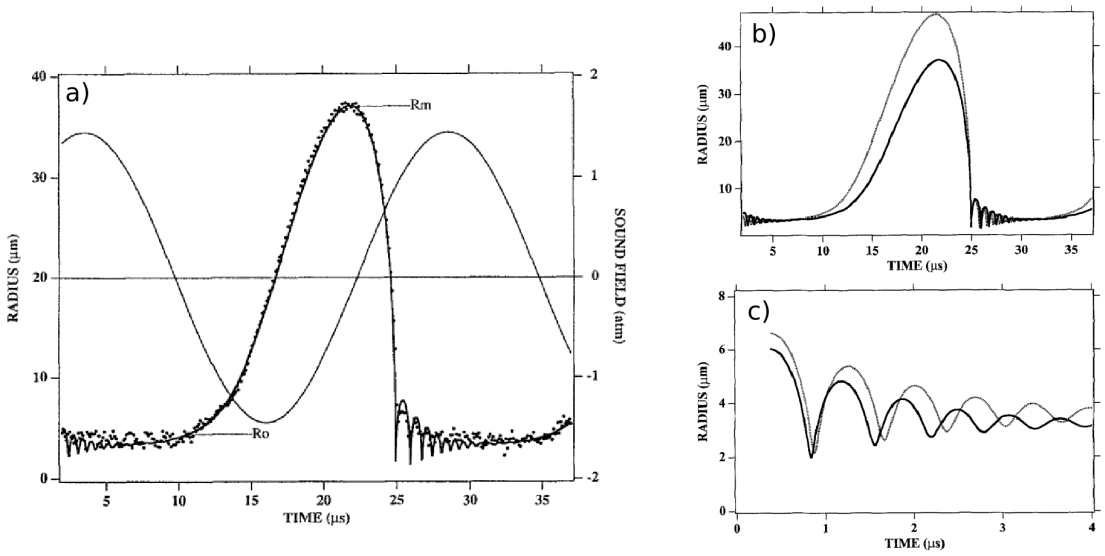

FIG. 4. Numerical solution of the $\propto \dot{p}_g$ RP equation variant discussed earlier with the gas dynamics given by the simple form in eq. 8. The dots are experimental results from Mie scattering [40, 50].

small jet of water into the flask (like our shrimp friends!) or blasting the water with a laser to boil a small volume [24, 29]. The later method is preferred as it enables more precise control over the initial bubble's radius.

Now let's discuss two experimentally accessible quantities that have turned out the be important. (i) The bubble's radius may be measured by *Mie scattering* and compared directly to solutions of the RP equations, allowing us to infer $T(t)$ by fitting to experiment [5, 40, 50]. (ii) The the light can be analyzed with a spectrometer, giving us information on the bubble's contents: in principle, we can learn about temperature and pressure inside the bubble, with spectral lines telling us about matter [18, 23, 28, 45]. We will look at this in the next section.

Mie scattering measurements scatter a laser off a bubble and analyze the scattered intensity. Assuming the bubble is a homogeneous dielectric sphere [33], the angular distribution of light scattered from the bubble at *fixed radius* and the time-dependent scattering off the bubble at *fixed angle* allow use to accurately measure the bubble's radius as a function of time [5]. A typical Mie scattering experiment is shown in fig. 3 (c). Parameters used to calculate the gas dynamics in the bubble are fit to the measured radius to build a full model of the dynamics. This procedure allows us to "measure" the temperature of a bubble undergoing SBSL. More accurate treatments of the gas dynamics from numerically solving the gas's NS equations are qualitatively in good agreement with these simpler model calculations [5, 29]. They are, however, in better quantitative agreement when their results are used to calculate the light spectrum [23–28]. Let us turn to discuss the

light's spectrum now.

IV. LET THERE BE LIGHT!

An important requirement for models of the light emission is *local thermodynamic equilibrium* (LTE). LTE is required for many reasons, foremost being the definition of temperature. LTE is expected to be true in a bubble undergoing SBSL since the particle density, $\sim 10^{28}/m^3$, and temerature, $\sim 10^4$ K, guarantee collisions between particles occur so frequently that equilibrium is ensured [5, 41, 51].

Any ensemble of atoms at a well defined temperature will emit radiation according to Planck's law. In the case of SBSL, we will look for corrections due to interactions of the emitted photons with atoms on the way out of the bubble [41]. Since we are assuming LTE, the intensity of emitted radiation depends instantaneoisly on the temperature-time curve, $T(t)$, that we just learned how to calculate. Planck's law gives the energy radiated per unit-time and unit-volume, I_B, [46]

$$I_B(\lambda; T(t)) = \frac{2hc^2}{\lambda^5} \frac{1}{\exp(hc/\lambda k_B T(t)) - 1}. \tag{10}$$

The subscript B is to remind us this is for a black-body; this is an *optically thick* thick bubble with "perfect" emission from the bubble's surface. Calculations of SBSL assuming black-body radiation over-estimate the number of photons emitted by orders of magnitude [5, 45]. Instead, we need to consider that the bubble has finite opacity.

Let's call the absorption coefficient $\kappa(\lambda, T(t))$ where we allow dependence on both wavelength λ and temperature, $T(t)$. Then the intensity of light that has travelled a distance s through the bubble is denoted by [45, 52, 53]

$$I(\lambda; T(t)) = I_B(\lambda; T(t)) \left(1 - \exp\left[-\kappa(\lambda; T(t))s\right]\right) \tag{11}$$

where have continued with the approximation that the temperature in the bubble is uniform [41, 45]. In the limit that $\kappa \to \infty$, we recover the result for a black-body emitter. On the otherhand, for a nearly tranparent bubble, $1 - \exp(\kappa s) \approx \kappa s$ and $I \approx I_B \kappa s$, i.e. the number of photons emitted is greatly reduced, a result that we require. For more complicated $\kappa(\lambda; T(t))$ (that may even depend on *position* through $T(\boldsymbol{x}, t)$ in a more accurate gas dynamical model) eq. 11 is integrated numerically. Integrating over the bubbles volume and over time allows calculating the radiated power spectrum which may be directly compared to experiment. A great deal of work has been devoted to identifying the relevant absorption mechanisms leading to κ, with most progress being made only after SBSL was discovered in aqueous H_2SO_4 [5, 23–28, 41, 45, 51].

What is now known is that the radiative processes occurring during SBSL depend very sensitively on the fluid properties and driving pressure [23, 28]. Due to its different mechanical properties, H_2SO_4 can support SBSL over a larger range of driving pressures than water [25]. For low driving pressures, the temperature and pressure are much lower than those encountered in bubbles in water and *discrete* emission lines for molecular dissociation and electronic transitions are directly observable [23, 28]. At larger driving pressures leading to bubble conditions comparable to those in water, however, what was found is that the *continous* processes electron-ion bremsstrahlung, electron-atom bremsstrahlung, and electron-ion recombination dominate [24, 29, 45, 52]. Moreover, it is now known that recombination of water-vapor molecules for SBSL in water is an important source of absorption, though this effect is limited by the small amount of these species in the bubble (see the argon rectification hypothesis above) [27].

Let us discuss SBSL of a *pure* Ar bubble in water. At the very high temperatures that occur in the bubble, a large fraction of (outer-shell) electrons are in excited states or are ionized from thier atoms completely [52]. Moreover, at the very high temperature and pressures in the bubble ($\sim 10^4$ K, $\sim$GPa), collisions between the particles are frequent. When an ionized electron passes near an atom or (not so near) an ion, it is deflected by the atom's potential. The deflection accelerates the electron, changing its kinetic energy. Since the mass of the ion or atom is much greater than the mass of the electron, we can take the atom or ion to be fixed. Since the electron is charged (and energy is conserved), it emits radiation through *bremsstrahlung* as its kinetic energy changes [33, 52]. It is also possible for the electron to become *bound* to the ion, emitting light to lower its kinetic energy.

The Saha equation of astrophysics allows us to estimate the fraction of particles that are ionized at a given temperature [27, 45, 52]

$$\frac{N_+ N_e}{N} \approx \left(\frac{2\pi m_e k_B T}{h^2}\right)^{3/2} \exp\left(-\frac{E_{ion}}{k_B T}\right) \tag{12}$$

It turns out that at typical SBSL temperatures, only $\sim 1\%$ of the atoms are ionized and thus, since collisions are very frequent, electron-atom bremsstrahlung is as important as electron-ion processes [23, 27, 45].

For electron-ion collision, the potential leading to bremsstrahlung is the long range Coulumb interaction. Below, we will derive a classical formula which is the most commonly used expressions in the context of SBSL. For electron-atom collisions, the potential is short range and the emission is very sensitive to the potential. The best route is numerical calculations with pseudopotentials [54], though classical approximations similar to the one we will derive below have been used too

[41, 45, 52]. Full quantum calculations of electron-ion bremsstrahlung absorption have also been done (see ref. for a review [55]).

The instantaneous radiation energy emitted by an electron is[6] [52, 56]

$$S(t) = \frac{2e^2}{3c^2}\boldsymbol{a}^2(t) \tag{13}$$

where $\boldsymbol{a}$ is the acceleration, e the electron charge, and c the speed of light (we are using CGS units here). This can be deduced by calculating the Poynting vector and finding the terms that don't vanish at infinite distance. If we Fourier transform $\boldsymbol{a}(t) \rightarrow \boldsymbol{a}(\nu)$, this becomes

$$S(\nu) = \frac{16\pi^2 e^2}{3c^2}\boldsymbol{a}^2(\nu) \tag{14}$$

with $\nu = c/\lambda$ the ordinary frequency.

Now consider a parallel beam of electrons with initial velocity v, and impact parameter b, incident from infinity with constant number density N_e. Integrating over the azimuthal angle, there are $vN_e \cdot 2\pi bdb$ electrons passing per unit time through a ring with area $2\pi bdb$ centered on the ion. Integrating over all possible orbits, the energy radiated *per-ion* per frequency interval $\nu + d\nu$, for unit electron flux, $vN_e = 1$, is the so-called "effective radiation" $d\epsilon_\nu$ [52]

$$d\epsilon_\nu = d\nu \int_0^\infty S(\nu) 2\pi b db. \tag{15}$$

This can be integrated for the motion of electron in the field of an ion with charge Ze to give [52, 57]

$$d\epsilon_\nu = \frac{32\pi^2}{3\sqrt{3}} \frac{Z^2 e^6}{m^2 c^3 v^2} d\nu \tag{16}$$

Now suppose that, in a unit-volume of gas, there are N_+ ions with charge Ze and N_e electrons with velocities distributed according to $f(v)dv = 4\pi(m/2\pi k_B T)^{3/2} \exp(-mv^2/2k_B T)v^2 dv$, i.e. the *Maxwell velocity distribution*. The energy emitted per unit-volume and unit-time in the frequency interval $\nu + d\nu$ by the electrons moving throught the field of the ions is

$$N_+ N_e v f(v) dv d\epsilon_\nu. \tag{17}$$

Note, we are assuming the velocity of the ions is neglibigle and that there is no recoil. The energy emitted by all of the electrons is obtained by integrating from v_{min} to $v = \infty$, with v_{min} satisfying

[6] This is evaluated on the surface of a sphere at a very large distance from the electron; the time, t, should be the retarded time. But since we are going to look at spectral properties, we won't worry about this detail.

$1/2 m_e v_{min}^2 = h\nu$. v_{min} is the minimum velocity of an electron that won't become bound. Using eq. 16 and integrating, we find the emission coefficient, j_ν, due to electron-ion bremsstrahlung:

$$j_\nu d\nu = \frac{32\pi}{3}\left(\frac{2\pi}{3k_B T m_e}\right)^{1/2}\frac{Z^2 e^6}{m_e c^3} N_+ N_e \exp\left(-\frac{h\nu}{k_B T}\right) d\nu. \tag{18}$$

This is a nice result, but we want the *absorption coefficient*. Following nearly identical arguments, the energy in the interval $\nu + d\nu$ *absorbed* per unit-volume and unit-time is

$$N_+ N_e \cdot I_B(\nu; T) d\nu \cdot f(v) dv \cdot a_\nu \left[1 - \exp\left(-\frac{h\nu}{k_B T}\right)\right]. \tag{19}$$

Here, a_ν is the absorption per-ion for electonrs velocity v and the factor $(1 - \exp[-h\nu/k_B T])$ accounts for effective decrease in absorption due to stimulated emission [52]. In equilibrium, which we assume in SBSL, total emission is exactly cancled by absorption. Then we set eq. 17 equal to eq. 19 to solve for a_ν. Integrating eq. 19 over v, we finally arrive at the spectral absorption coeffecient for a gas of electrons and ions with number densisites N_e and N_+ respectively

$$\kappa_\nu = \frac{4}{3}\left(\frac{2\pi}{3m_e k_B T(t)}\right)^{1/2}\frac{Z^2 e^6}{hcm_e \nu^3} N_+ N_e. \tag{20}$$

In terms of the wavelength, λ, and in SI units, we arrive at the equation used to calculate the SBSL spectrum in nearly all modern work [25–27, 45]

$$\kappa_\lambda = \frac{4}{3}\left(\frac{2\pi}{3m_e k_B T(t)}\right)^{1/2}\frac{Z^2 e^6 \lambda^3}{(4\pi\epsilon_0)^3 hc^4 m_e} N_+ N_e. \tag{21}$$

With this (and expressions for other absorption mechanisms [25, 45, 52]) we finally have a complete model for SBSL in water!

V. SUMMARY AND OUTLOOK

We could now perform a full calculation of the light spectrum in SBSL; let's sketch it here: an RP equation (e.g. eq. **??**) is combined with a gas-dynamical equation (e.g. eq. 8) and the radius-time curve $R(t)$ of bubble undergoing SBSL is calculated numerically, also giving us the temperature as a function of time, $T(t)$ (e.g. eq. 9). We use eq. 12 to determing the fraction of ions and electrons present and eq. 21 gives us the amount of light absorbed by electron-ion bremsstrahlung, with similar expressions for electron-atom bremsstrahlung [54] and electron-ion recombination [25–27, 45, 52]. These equations and eq. 11 for the energy radiated in the bubble give us the power spectrum as a function of $T(t)$ and the power spectrum can be directly compared to experiment. Calculations from almost exactly these lines are how SBSL was explained in water [5, 29, 41, 45].

Assuming different absorption mechanisms for lower temperatures and directly solving the full gas dynamical NS equations for SBSL in 85% aqueous H_2SO_4, the SBSL has also been calculated nearly perfectly [25–27]. Early work on SBSL ignored bound-bound transitions since lines weren't observed in the SBSL spectrum in water. It was that they would be very broad due to the extremely high pressure in the bubble, but estimated broadening was too small to lead to what was seen in experiment and it was concluded instead that these process don't occur [41, 45]. Later work using more accurate gas dyanmical models have shown that bound-bound transitions are important too, with emission lines visible at the lower pressures in SBSL in aqueous H_2SO_4 [26, 27] and, when correctly including the broadening, pretty much all features of SBSL spectra in water and aqueous H_2SO_4 are predicted correclty [23, 24, 28]. SBSL is a solved problem!

VI. ACKNOWLEDGMENTS

Appendix A: Electrical Arguments

Appendix B: The Casimir Argument

[1] M. Versluis, B. Schmitz, A. Von der Heydt, and D. Lohse, How snapping shrimp snap: through cavitating bubbles, Science **289**, 2114 (2000).

[2] D. Lohse, B. Schmitz, and M. Versluis, Snapping shrimp make flashing bubbles, Nature **413**, 477 (2001).

[3] X. Tang and D. Staack, Bioinspired mechanical device generates plasma in water via cavitation, Science advances **5**, eaau7765 (2019).

[4] F. A. Everest, R. W. Young, and M. W. Johnson, Acoustical characteristics of noise produced by snapping shrimp, The Journal of the Acoustical Society of America **20**, 137 (1948).

[5] M. P. Brenner, S. Hilgenfeldt, and D. Lohse, Single-bubble sonoluminescence, Reviews of modern physics **74**, 425 (2002).

[6] L. A. Crum and R. A. Roy, Sonoluminescence, Science **266**, 233 (1994).

[7] D. F. Gaitan, L. A. Crum, C. C. Church, and R. A. Roy, Sonoluminescence and bubble dynamics for a single, stable, cavitation bubble, The Journal of the Acoustical Society of America **91**, 3166 (1992).

[8] N. Marinesco and J. Trillat, Actions des ultrasons sur les plaques photographiques, Proceedings of the Royal Academy of Science **196**, 858 (1933).

[9] H. Frenzel and H. Schultes, Luminescenz im ultraschallbeschickten wasser, Zeitschrift für Physikalische Chemie **27**, 421 (1934).

[10] S. Li, C. E. Brennen, and Y. Matsumoto, Introduction for amazing (cavitation) bubbles (2015).

[11] L. Rayleigh, On the pressure developed in a liquid during the collapse of a spherical cavity: Philosophical magazine series 6, 34, 94–98 (1917).

[12] M. S. Plesset and A. Prosperetti, Bubble dynamics and cavitation, Annual review of fluid mechanics **9**, 145 (1977).

[13] A. Prosperetti, Old-fashioned bubble dynamics, Sonochemistry and sonoluminescence , 39 (1999).

[14] R. Löfstedt, K. Weninger, S. Putterman, and B. P. Barber, Sonoluminescing bubbles and mass diffusion, Physical Review E **51**, 4400 (1995).

[15] B. P. Barber, R. Hiller, K. Arisaka, H. Fetterman, and S. Putterman, Resolving the picosecond characteristics of synchronous sonoluminescence, The Journal of the Acoustical Society of America **91**, 3061 (1992).

[16] D. F. Gaitan, *An experimental investigation of acoustic cavitation in gaseous liquids*, Ph.D. thesis, The University of Mississippi (1990).

[17] D. Lohse, Bubble puzzles: From fundamentals to applications, Physical review fluids **3**, 110504 (2018).

[18] R. Hiller, S. J. Putterman, and B. P. Barber, Spectrum of synchronous picosecond sonoluminescence, Physical review letters **69**, 1182 (1992).

[19] R. Hiller, K. Weninger, S. J. Putterman, and B. P. Barber, Effect of noble gas doping in single-bubble sonoluminescence, Science **266**, 248 (1994).

[20] B. P. Barber and S. J. Putterman, Observation of synchronous picosecond sonoluminescence, Nature **352**, 318 (1991).

[21] C. Wu and P. H. Roberts, Shock-wave propagation in a sonoluminescing gas bubble, Physical review letters **70**, 3424 (1993).

[22] H. P. Greenspan and A. Nadim, On sonoluminescence of an oscillating gas bubble, Physics of Fluids A: Fluid Dynamics **5**, 1065 (1993).

[23] D. J. Flannigan and K. S. Suslick, Plasma formation and temperature measurement during single-bubble cavitation, Nature **434**, 52 (2005).

[24] K. S. Suslick and D. J. Flannigan, Inside a collapsing bubble: sonoluminescence and the conditions during cavitation, Annu. Rev. Phys. Chem. **59**, 659 (2008).

[25] Y. An and C. Li, Diagnosing temperature change inside sonoluminescing bubbles by calculating line spectra, Physical Review E **80**, 046320 (2009).

[26] Y. An and C. Li, Spectral lines of oh radicals and na atoms in sonoluminescence, Physical Review E **78**, 046313 (2008).

[27] Y. An, Mechanism of single-bubble sonoluminescence, Physical Review E **74**, 026304 (2006).

[28] D. J. Flannigan, S. D. Hopkins, C. G. Camara, S. J. Putterman, and K. S. Suslick, Measurement of pressure and density inside a single sonoluminescing bubble, Physical review letters **96**, 204301 (2006).

[29] K. Yasui, *Acoustic cavitation and bubble dynamics* (Springer, 2018).

[30] A. Prosperetti and A. Lezzi, Bubble dynamics in a compressible liquid. part 1. first-order theory, Journal of Fluid Mechanics **168**, 457 (1986).

[31] C. E. Brennen, *Cavitation and bubble dynamics* (Cambridge University Press, 2014).

[32] M. S. Plesset, The dynamics of cavitation bubbles, (1949).

[33] J. D. Jackson, Classical electrodynamics (1999).

[34] T. Leighton, Derivation of the rayleigh-plesset equation in terms of volume, (2007).

[35] J. B. Keller and M. Miksis, Bubble oscillations of large amplitude, The Journal of the Acoustical Society of America **68**, 628 (1980).

[36] K. Yasui, Dynamics of acoustic bubbles, in *Sonochemistry and the Acoustic Bubble* (Elsevier, 2015) pp. 41–83.

[37] A. Prosperetti, L. A. Crum, and K. W. Commander, Nonlinear bubble dynamics, The Journal of the Acoustical Society of America **83**, 502 (1988).

[38] J. B. Keller and I. I. Kolodner, Damping of underwater explosion bubble oscillations, Journal of applied physics **27**, 1152 (1956).

[39] A. Lezzi and A. Prosperetti, Bubble dynamics in a compressible liquid. part 2. second-order theory, Journal of Fluid Mechanics **185**, 289 (1987).

[40] B. P. Barber, R. A. Hiller, R. Löfstedt, S. J. Putterman, and K. R. Weninger, Defining the unknowns of sonoluminescence, Physics Reports **281**, 65 (1997).

[41] S. Hilgenfeldt, S. Grossmann, and D. Lohse, Sonoluminescence light emission, Physics of fluids **11**, 1318 (1999).

[42] K. Weninger, R. Hiller, B. P. Barber, D. Lacoste, and S. J. Putterman, Sonoluminescence from single bubbles in nonaqueous liquids: new parameter space for sonochemistry, The Journal of Physical Chemistry **99**, 14195 (1995).

[43] D. Lohse, M. P. Brenner, T. F. Dupont, S. Hilgenfeldt, and B. Johnston, Sonoluminescing air bubbles rectify argon, Physical review letters **78**, 1359 (1997).

[44] R. Löfstedt, B. P. Barber, and S. J. Putterman, Toward a hydrodynamic theory of sonoluminescence, Physics of Fluids A: Fluid Dynamics **5**, 2911 (1993).

[45] S. Hilgenfeldt, S. Grossmann, and D. Lohse, A simple explanation of light emission in sonoluminescence, Nature **398**, 402 (1999).

[46] D. V. Schroeder, An introduction to thermal physics (1999).

[47] S. Sivasubramanian, A. Widom, and Y. Srivastava, Temperature of a compressed bubble with application to sonoluminescence, arXiv preprint cond-mat/0207465 (2002).

[48] B. Gompf and R. Pecha, Mie scattering from a sonoluminescing bubble with high spatial and temporal resolution, Physical Review E **61**, 5253 (2000).

[49] W. Lentz, A. A. Atchley, and D. F. Gaitan, Mie scattering from a sonoluminescing air bubble in water, Applied optics **34**, 2648 (1995).

[50] B. P. Barber and S. J. Putterman, Light scattering measurements of the repetitive supersonic implosion of a sonoluminescing bubble, Physical review letters **69**, 3839 (1992).

[51] K. Yasui, Mechanism of single-bubble sonoluminescence, Physical review E **60**, 1754 (1999).

[52] Y. B. Zel'Dovich and Y. P. Raizer, *Physics of shock waves and high-temperature hydrodynamic phenomena* (Courier Corporation, 2002).

[53] R. L. Taylor and G. Caledonia, Experimental determination of the cross-sections for neutral bremsstrahlung: I. ne, ar and xe, Journal of Quantitative Spectroscopy and Radiative Transfer **9**, 657 (1969).

[54] S. Geltman, Free-free radiation in electron-neutral atom collisions, Journal of Quantitative Spectroscopy and Radiative Transfer **13**, 601 (1973).

[55] M. Eckert, From aether impulse to qed: Sommerfeld and the bremsstrahlen theory, Studies in History and Philosophy of Science Part B: Studies in History and Philosophy of Modern Physics **51**, 9 (2015).

[56] D. J. Griffiths, Introduction to electrodynamics (2005).

[57] L. D. Landau, *The classical theory of fields*, Vol. 2 (Elsevier, 2013).